

## Formulation without Ultrafine Coke Particles: A Way to Increase the Features of the Carbon Anode

F. Chevarin<sup>1</sup>, R. Ishak<sup>2</sup>, G. Rouget<sup>3</sup>, D. Ziegler<sup>4</sup>, M. Fafard<sup>5</sup>, H. Alamdari<sup>6</sup>

1. Postdoctoral Fellow

2. Ph.D. student

3. Ph.D. student

6. Professor

Department of Mining, Metallurgical and Materials Engineering, Université Laval, Québec, Canada

5. Professor

Department of Civil Engineering, Université Laval, Québec, Canada

1. Research assistant

2. Ph.D. student

3. Ph.D. student

5. Professor

6. Professor

NSERC/Alcoa Industrial Research Chair MACE<sup>3</sup> and Aluminum Research Centre – REGAL  
Université Laval, Québec, Canada

4. Carbon manager

Alcoa Primary Metals, Alcoa Technical Center, Pittsburgh, USA

Corresponding author: houshang.alamdari@gmn.ulaval.ca

### Abstract

Carbon anode properties (reactivity and electrical resistivity) may affect the anode lifetime in the Hall-Héroult cell. In order to extend the anode lifetime a number of solutions have been proposed. Some of them include the appropriate choice of the raw materials (coke, anthracite, etc.), the optimization of the manufacturing process and the adjustment of the anode formulation. In this work, removing the ultrafines fraction from the coke was proposed, aiming at reducing the air and CO<sub>2</sub> reactivity of the anode. Dry sieving of the fine fraction with 37, 45 and 53 μm sieves allowed removing the finest particles from the coke recipe. The replacement of the ultrafines by a same amount of larger particles within the fine fraction and by some adjustments such as the pitch content, revealed the effects of ultrafine removal on the gas reactivity and electrical resistivity of anodes. A decrease of the apparent density and an augmentation of the electrical resistivity of the modified recipe were noticed, whereas the dusting during the reactivity tests was reduced.

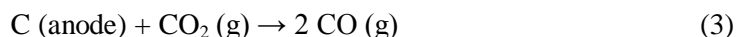
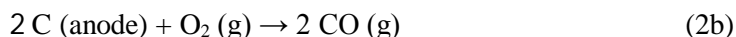
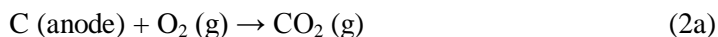
**Keywords:** ultrafine coke particles, apparent density, air and CO<sub>2</sub> reactivity, electrical resistivity, dusting phenomenon.

### 1 Introduction

Primary aluminum is produced by reduction of alumina (Al<sub>2</sub>O<sub>3</sub>) in an electrolysis cell at 960 °C according to the Hall-Héroult process (Equation 1). The cell is made of carbon anodes, carbon cathode and molten cryolite as electrolyte. The anode is composed of calcined petroleum coke (with different particle sizes), recycled anodes (butts) and coal-tar-pitch.



According to the stoichiometric reduction reaction of alumina, 334 kg of carbon is theoretically required to produce one ton of aluminum. However, the real consumption of carbon (in electrolysis cell at an industrial scale) is about 415 kg per ton of aluminum [1]. This overconsumption of carbon is essentially due to the reversibility of the reduction reaction, as well as the anode gasification with air, Eq. (2a, 2b) and CO<sub>2</sub>, Eq. (3) [2-5].



An empirical model was proposed by Fisher *et al.* [6] to reveal the importance of the anode properties on its overconsumption in the electrolysis pots; Purity, Structure and Porosity model (PSP). No mathematical formula has been assigned to this model as of this date. Several studies have been published to determine precisely the essential anode features affecting the carbon overconsumption caused by the three abovementioned chemical reactions (Eq. 2a, 2b and 3). A number of parameters were identified as important factors affecting the anode overconsumption such as the level of impurities [7-10], the graphitization level (related to the final temperature and the soaking time during baking) [2, 11-14], the anode porosity, the apparent density and the pore size distribution [4, 15-18]. Some of these features could be adjusted by modifying of the anode manufacturing steps such as the vibration time or the soaking time during baking [2, 3, 19]. In the same way, anode formulation could be modified to optimize the anode quality and to decrease its overconsumption.

The anode formulation could be adjusted with the variation of the pitch content [20-24], the fraction of butts [5, 25-27] and the particle size distribution of coke [28-34]. The size distribution of coke is roughly divided in coarse (+ 74 μm) and fine fractions. The fine fraction of coke particles is important to increase the vibrated bulk density (VBD) [35-37], to improve the compaction behavior of the anode paste [23, 28, 38], thus increasing the apparent density and the mechanical properties of anode [28, 33, 34] and decreasing its air and CO<sub>2</sub> reactivity [30] as well as its electrical resistivity.

In the industrial practice, the fineness of coke particles is determined by the Blaine Number (BN). The BN is related to the external surface area of the particles, and consequently to the particle size distribution. A high BN of a coke recipe indicates that it contains higher fraction of fine particles. A high BN (superior to 4000) could significantly increase the air and CO<sub>2</sub> reactivity as well as the pitch demand. This would result in an augmentation of the total anode cost [34]. Therefore, a balance must be respected to determine the optimal fineness of the coke particles. On the one hand, the apparent density of anode increases and its porosity and permeability decreases with a high BN, resulting in a decrease of air and CO<sub>2</sub> reactivity. On the other hand, a higher fineness generates a high surface area of coke particles, increasing the reactivity of coke particles and dusting [39, 40].

The aim of this work is to reveal the effect of ultrafine fraction of the coke recipe on the anode properties; i.e. air reactivity, dusting and electrical resistivity. Considering the review about the fineness of coke in the anode formulation, a new particle size distribution is proposed. The fine fraction of the coke recipe was modified by removing the ultrafine particles and replacing them with the coke in the range of upper limit of fine fractions. Several adjustments were carried out in order to maintain the paste properties such as the weight substitution of sub-fraction by an equivalent amount of the “truncated fraction”.

## 2 Experimental procedure

### 2.1 Materials

The raw materials were provided by Deschambault aluminum smelting plant (Alcoa, Canada). Lab scale prebaked anodes were fabricated following the typical formulation used in laboratory anode manufacturing process. In Table 1, the chemical composition of the raw materials, i.e. calcined coke and coal-tar-pitch, are detailed. To prepare the fine fraction of the anode recipe, 2 kg of coke particles (-8 + 16 US Mesh; -2.38 + 1.19 mm) was milled in a ball mill with steel balls during 36 minutes. The rotation speed of the mill was approximately 60 rpm. A measured Blaine Number of  $4166 \pm 174$  was obtained for the milled particles using conditions described previously [41]. The fine fraction (4166 BN) has been sieved to separate 4 sub-fractions of the fines (Table 2). The size fractions of the coke particles used in anode recipe are presented in Table 3 and Table 4. The Blaine Number (BN) was measured with laser diffraction particle size analyzer (Malvern Mastersizer 2000); the BN is a number associated at the specific surface area (SSA) and is used to assess the fineness of the powder [38].

The anode paste was prepared by preheating coke particles at 185 °C for 90 minutes, then the binder-pitch (16.2 wt.%) was added to coke and heated for 30 minutes. Finally, the blend was mixed at the same temperature for 10 minutes and then pressed at 150 °C during 3 minutes by applying a uniaxial pressure of 70 MPa [19, 23, 41]. This final product, called green anode, had a diameter of 50 mm and an approximate height of 100 mm. Prior to baking in a muffle furnace, the green anodes were placed in an inconel® box and covered by coke particles in order to protect them against air oxidation. The heating program was as follow: from room temperature to 150 °C at a heating rate of 60 °C/h, then from 150 °C to 650 °C at a rate of 20 °C/h, and finally from 650 °C to 1100 °C at 50 °C/h. This was followed by a soaking time of 20 hours at 1100 °C. At the end of this process, the furnace was switched off and allowed to cool to room temperature.

**Table 1. Chemical composition of calcined coke and coal tar pitch.**

Properties	S (wt %)	Na (ppmw)	Si (ppmw)	Ca (ppmw)	V (ppmw)	Fe (ppmw)	Ni (ppmw)
Calcined coke	$2.13 \pm 0.06$	$100 \pm 7$	$120 \pm 17$	$130 \pm 7$	$360 \pm 18$	$460 \pm 23$	$250 \pm 13$
Coal tar pitch	$0.55 \pm 0.02$	$48 \pm 3$	$254 \pm 36$	$71 \pm 4$	N/A	$209 \pm 10$	N/A

**Table 2. Particle size distribution of calcined coke (wt. %) of the fine fraction obtained by ball milling (4166 BN); the BN was measured with the Malvern software.**

Particle sizes (US Mesh)	Superior Inferior	+50	-50 +100	-100 +200	-200 +270	-270 +325	-325 +400	-400
Particle sizes ( $\mu\text{m}$ )	Superior Inferior		-297 +149	-149 +74	-74 +53	-53 +45	-45 37	-37
Coke (wt. %)		0.0	5.4	48.5	27.9	2.7	1.6	13.7

**Table 3. Particle size distribution of calcined coke (wt. %) used for the preparation of the dry mixture used for the fabrication of prebaked anodes.**

Particle sizes (US Mesh)	Superior	-4	-8	-14	-28	-50	-100	Fraction obtained by ball milling
	Inferior	+8	+14	+28	+50	-100	-200	
Particle sizes ( $\mu\text{m}$ )	Superior	-4760	-2380	-1410	-595	-297	-149	-297
	Inferior	+2380	+1410	+595	+297	+149	+74	+0.01
Initial particle size distribution		22.0	10.1	11.5	12.7	8.8	10.8	24.2

**Table 4. Particle size distribution of calcined coke (wt. %) used for the preparation of the dry mixture including the 2 different fractions (coarse and fine fractions) of the ball milled mixture.**

Type of Fractions		Coarse fraction					
Particle sizes (US Mesh)	Superior	-4	-8	-14	-28	-50	-100
	Inferior	+8	+14	+28	+50	+100	+200
Particle sizes ( $\mu\text{m}$ )	Superior	-4760	-2380	-1410	-595	-297	-149
	Inferior	+2380	+1410	+595	+297	+149	+74
Initial particle size distribution		22.0	10.1	11.5	12.7	8.8	10.8

Type of Fractions		Fine fraction					
Particle sizes (US Mesh)	Superior	-50	-100	-200	-270	-325	-400
	Inferior	+100	+200	+270	+325	+400	
Particle sizes ( $\mu\text{m}$ )	Superior	-297	-149	-74	-53	-45	-37
	Inferior	+149	+74	+53	+45	+37	
Initial particle size distribution		1.3	11.8	6.8	0.7	0.4	3.3

## 2.2 Truncated fine fraction preparation

In order to modify the size distribution of the fine fraction (4166 BN) obtained by ball milling, a dry sieving was carried out. Three sieves were used to subdivide the fine fraction: +37  $\mu\text{m}$  (400 US Mesh), +45  $\mu\text{m}$  (325 US Mesh) and +53  $\mu\text{m}$  (270 US Mesh). The sieving was performed under dry conditions. The particles remained above the sieve are the particles of the truncated fine fraction and the particles passing through the sieve are considered as ultrafines. The modified recipes of anode were made by these “truncated” fine fractions.

## 2.3 Samples characterization

Two reactivity tests, i.e.  $\text{CO}_2$  and air reactivity, were used.  $\text{CO}_2$  reactivity test was performed according to the standard ISO 12988-2. The anode sample with a diameter of 50 mm and a length of 60 mm was gasified under a  $\text{CO}_2$  flow (200 l/h) during 7 hours at 960 °C. Three results were obtained with this test; the residue corresponding to the mass loss in percentage after the test, the dust quantity in percentage associated to the detachment of the carbon particles during the test and the loss related to the mass loss of the sample in gas state (CO molecules). Air reactivity tests were performed according the standard ISO 12989. The samples were exposed at a temperature of 550 °C under an airflow and a cooling of the furnace was applied with a cooling rate of 15 °C/h. The duration time was 10 hours. The three previous parameters (Residue, Dust and Loss) were analyzed for the air test as well.

The crystallite size ( $L_c$ ) and the level of impurities were measured by XRD (Phillips, PW 1800 following the ISO standard 20203) and by XRF (PANalytical Axios max according to the ASTM D4326-06 standard) spectrometers, respectively. The apparent density of the anode samples were measured according to the ISO 12985-1.

Electrical resistivity measurements were performed using the Van-der-Pauw method (VdP) [42, 43]. This technique allows measuring the intrinsic electrical resistivity of the material regardless of the surface and structural defects [44]. The electrical resistivity of each sample was measured four times, then averaged. Each measurement was performed with a 45° rotation from the previous test. A 1 Amp current was applied and the voltage drop was measured to obtain an equivalent electrical resistance. Two measurements of equivalent resistances are required to obtain one value of electrical resistivity. The electrical resistivity of the sample was calculated according to the following Equation:

$$e^{-\pi \frac{d}{\rho} \cdot R_1} + e^{-\pi \frac{d}{\rho} \cdot R_2} = 1 \quad (4)$$

$R_1$  and  $R_2$  stand for the two contiguous equivalent resistances measured,  $\rho$  stands for the electrical resistivity, and  $d$  is the thickness of the sample. To perform measurements of electrical resistivity of circular samples with a better accuracy, Kasl and Hoch [45] recommend that the thickness of the sample remains smaller than its diameter. This condition was respected for all samples.

### 3 Results and discussion

#### 3.1 Optimization of the fineness of the fine fraction

The fine fraction of the coke with a BN of 4000, as obtained by ball milling, as well as the sieved fractions of the same batch were analysed for the particle size distribution (Figure 1). Under dry conditions, the separation of fine coke particles by sieving is efficient for the 37, 45 and 53  $\mu\text{m}$  sieves. Using the Malvern software, the Blaine Number was calculated for the three truncated samples (Table 5). It can be seen that when the particles smaller than 37  $\mu\text{m}$  are removed, the BN remains quite constant. This indicates that the BN of the fine fraction of coke recipe is essentially controlled by particles smaller than 37  $\mu\text{m}$ .

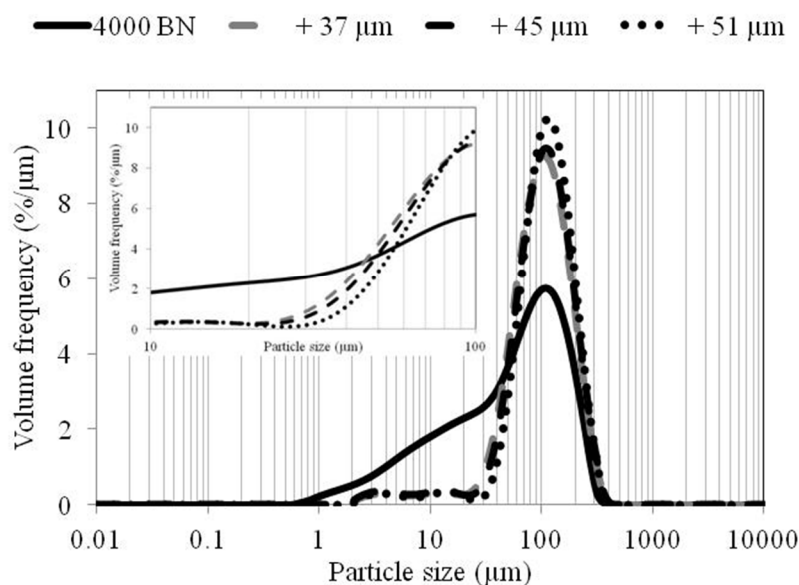


**Figure 1. Particle size distributions of the fine fractions remaining above the meshes (37, 45 and 53  $\mu\text{m}$ ) and the initial particle size distribution of the reference (4000 BN); analysis performed under dry condition on a Malvern instrument.**

**Table 5. Blaine Numbers of the truncated fine fraction.**

Size of the sieve ( $\mu\text{m}$ )	+37	+45	+53
Blaine Number (BN)	$1240 \pm 95$	$1281 \pm 33$	$1115 \pm 13$

The weight repartitions of the three truncated fine fractions (+ 37, + 45 and + 53  $\mu\text{m}$ ) are presented in Table 6. Sieves at 37, 45 and 53  $\mu\text{m}$  revealed that the ultrafine fraction represents between 35 and 46 wt. % of the fine coke.

**Table 6. Weight repartition for the three truncated fine fractions: 37, 45 and 53  $\mu\text{m}$ , from the ball milling fraction.**

Mesh size ( $\mu\text{m}$ )	Weight (wt. %) of the particles inferior than the mesh size (particles passing through the mesh)	Weight (wt. %) of the particles superior at the mesh size (particles remaining above the mesh)
37	$35 \pm 1$	$65 \pm 1$
45	$39 \pm 1$	$61 \pm 1$
53	$46 \pm 2$	$54 \pm 2$

Table 7 gives the particle size distributions of the three anode recipes; + 37, + 45 and + 53  $\mu\text{m}$ . In order to compensate for the removal of the particles passing through the sieves, a similar mass of the fraction remained above the sieves is added.

**Table 7. Particle size distribution of calcined coke (wt. %) for the three anode recipes without the finest fractions (+ 37, + 45 and + 53  $\mu\text{m}$ ).**

Type of Fractions		Coarse fraction					
Particle sizes (US Mesh)	Superior Inferior	-4 +8	-8 +14	-14 +28	-28 +50	-50 -100	-100 -200
Particle sizes ( $\mu\text{m}$ )	Superior Inferior	-4760 +2380	-2380 +1410	-1410 +595	-595 +297	-297 +149	-149 +74
Initial particle size distribution		22.0	10.1	11.5	12.7	8.8	10.8
+ 37 $\mu\text{m}$		22.0	10.1	11.5	12.7	8.8	10.8
+ 45 $\mu\text{m}$		22.0	10.1	11.5	12.7	8.8	10.8
+ 53 $\mu\text{m}$		22.0	10.1	11.5	12.7	8.8	10.8

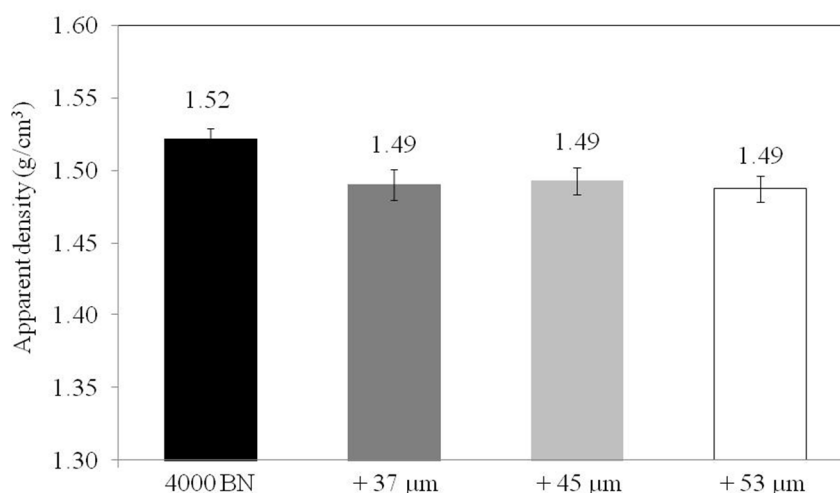
Type of Fractions		Fine fraction					
Particle sizes (US Mesh)	Superior Inferior	-50 +100	-100 +200	-200 +270	-270 +325	-325 -400	-400
Particle sizes ( $\mu\text{m}$ )	Superior Inferior	-297 +149	-149 +74	-74 +53	-53 +45	-45 +37	-37
Initial particle size distribution		1.3	11.8	6.8	0.7	0.4	3.3
+ 37 $\mu\text{m}$		1.5	13.6	7.8	0.8	0.4	0.0
+ 45 $\mu\text{m}$		1.6	13.9	8.0	0.8	0.0	0.0
+ 53 $\mu\text{m}$		1.6	14.3	8.3	0.0	0.0	0.0

Table 8 indicates the chemical compositions and structural property of the baked anodes made with four fine fractions; 4000 BN; 4000 BN without the ultrafine fraction sieved at 37, 45 and 53  $\mu\text{m}$ . All the elements and the graphitization height ( $L_C$ ) are similar for the four types of the baked anodes.

**Table 8. Chemical compositions and structural property of the baked anodes made with four fine fractions; 4000 BN and 4000 BN without the ultrafine fraction sieved at 37, 45, 53  $\mu\text{m}$ .**

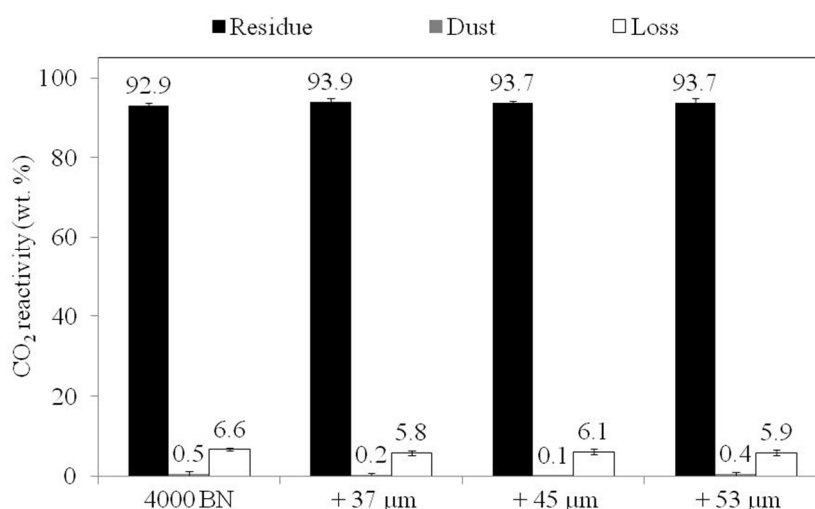
Properties	S (wt %)	Na (ppmw)	Ca (ppmw)	V (ppmw)	Fe (ppmw)	Ni (ppmw)	$L_C$ (nm)
4000BN	1.78 $\pm$ 0.09	170 $\pm$ 27	178 $\pm$ 21	336 $\pm$ 34	615 $\pm$ 61	207 $\pm$ 23	2.9 $\pm$ 0.1
+37 $\mu\text{m}$	1.76 $\pm$ 0.07	155 $\pm$ 27	169 $\pm$ 16	333 $\pm$ 20	628 $\pm$ 113	206 $\pm$ 13	3.0 $\pm$ 0.1
+45 $\mu\text{m}$	1.78 $\pm$ 0.05	156 $\pm$ 12	171 $\pm$ 9	328 $\pm$ 26	573 $\pm$ 53	201 $\pm$ 19	3.0 $\pm$ 0.1
+53 $\mu\text{m}$	1.77 $\pm$ 0.05	156 $\pm$ 17	170 $\pm$ 16	328 $\pm$ 16	592 $\pm$ 42	203 $\pm$ 14	3.0 $\pm$ 0.1

The apparent density of the modified anode recipe (with truncated fine fractions) was measured after the baking process in order to estimate the impact of the particle size distribution of the fine fraction. Three replicas were made for each recipe. Figure 2 shows that the reference samples with 4000 BN have a slightly higher apparent density (1.52  $\text{g}/\text{cm}^3$ ) compared to the samples with a truncated fine fraction (1.49  $\text{g}/\text{cm}^3$ ). The diminution of the apparent density by the ultrafine removal could be explained by the fact that the pores were not filled by the ultrafine particles. At an industrial scale, the apparent density is close to 1.6  $\text{g}/\text{cm}^3$ ; the gap could be explained by the presence of anode butts (materials with a high density) and the larger particles of coke (superior than 4.7 mm).



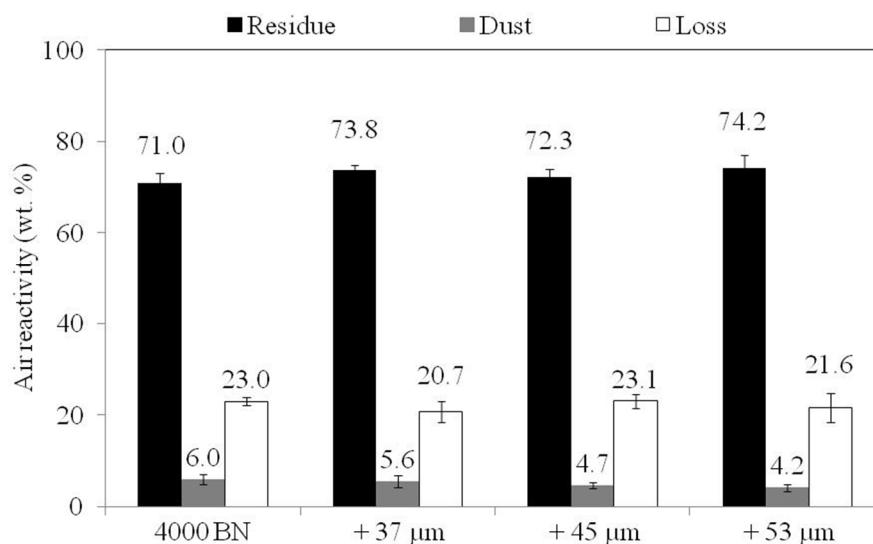
**Figure 2. Apparent density of the four anodes, made with four fine fractions; 4000 BN and 4000 BN without the ultrafine fraction sieved at 37, 45, 53 µm, measured in following the standard ISO 12985-1.**

Figure 3 presents the CO<sub>2</sub> reactivity of the baked anodes, made with four fine fractions; 4000 BN and 4000 BN without the ultrafine fractions sieved at 37, 45 and 53 µm. The CO<sub>2</sub> reactivity is expressed with three parameters; residue, dust and loss. Three anodes for each recipe were gasified to estimate the CO<sub>2</sub> reactivity. In Fig. 3, the percentage of residue (quantity of sample remaining after the test) is slightly higher for the truncated fine fraction anodes compared to 4000 BN reference anode. Moreover, the dust and loss percentages are lower for the truncated 4000 BN anodes. Considering a similar level of catalyst and inhibitor elements (Table 8) and a lower apparent density for the anodes with the ultrafine removal (Fig. 2); the CO<sub>2</sub> reactivity for all samples is similar. The ultrafine particles fill the small pores in the larger coke particles and between particles, increasing its apparent density. The ultrafine particles are more chemical active and their removal decreases the reactivity but their presence increases the apparent density (higher apparent density) and decreases the permeability. These two factors operate in opposite directions and, to some extent, neutralize their mutual effect.



**Figure 3. CO<sub>2</sub> reactivity of the four types of anodes, made with four fine fractions; 4000 BN and 4000 BN without the ultrafine fraction sieved at 37, 45, 53 µm, measured according to the standard ISO 12988.**

The results of air reactivity are presented as three separated parameters: residue, dust and loss. Figure 4 describes the air reactivity results for the four types of anodes, according to the standard ISO 12989-1. As for the CO<sub>2</sub> reactivity, the percentages of residue of the truncated fine fraction anodes are higher than that of the reference 4000 BN anode. Although the loss percentages are quite similar for the four types of anodes, the dust percentages are lower for the truncated fine fraction anodes. Consequently, the sieving and the substitution of the ultrafine fraction decrease dust emission. The dusting phenomenon is described by detachment of the coke particles from the anode block. This phenomenon is frequently explained by the higher reactivity of the binder matrix (mixture of pitch and fine coke particles) compared to the larger coke particles i.e. a selective oxidation of O<sub>2</sub> molecules with the binder matrix [21, 46]. Chevarin et al. [40] showed that the high reactivity of binder matrix could be explained by the high reactivity of fine coke particles and not by that of the pitch coke. Thus, the removal of ultrafine particles would limit the binder matrix reactivity by decreasing the surface area of the binder matrix (the finest particles have a larger surface area than the larger particles and it is assumed that not all the surface of the fine coke is covered by pitch).



**Figure 4. Air reactivity of the four types of anodes, made with four fine fractions; 4000 BN and 4000 BN without the ultrafine fraction sieved at 37, 45, 53 μm, measured according to the ISO standard 12989-1.**

The electrical resistivity measurements were performed on the four types of anodes, using VdP method [44]. As presented in the Figure 5, the electrical resistivity of the four samples is quite similar. Results show that the substitution of the finest particles by larger particles does not affect significantly the electrical resistivity of carbon anodes. This is accordance with the literature where it has been reported that the electrical resistivity is essentially controlled by particles larger than 100 US Mesh (75 μm) [47]. The slight increase in the resistivity could be attributed to the decrease in density.

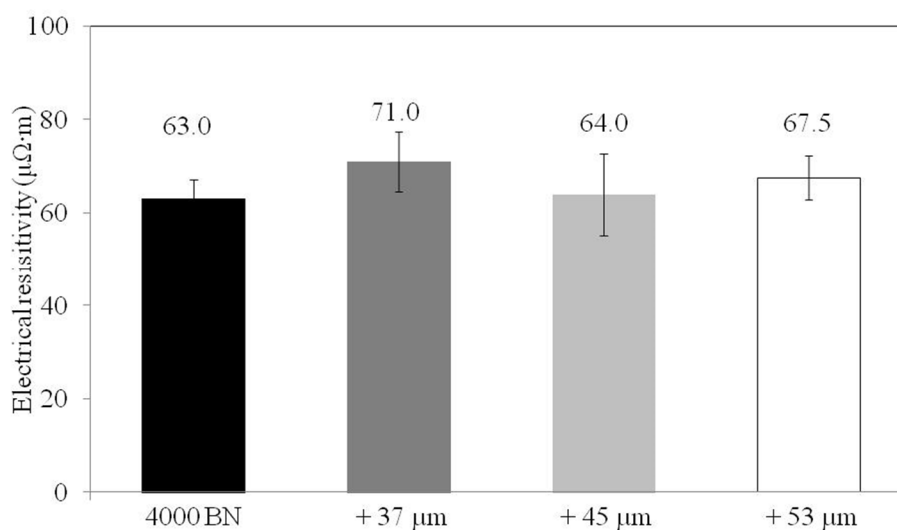


**Figure 5. Electrical resistivity of the four types of anodes, made with four fine fractions; 4000 BN and 4000 BN without the ultrafine fraction sieved at 37, 45, 53 μm, measured according to the four-probe method.**

### 3.2 Modification of the anode recipe

As seen so far, the substitution of the ultrafine particles in the fine fraction reduces dust emission under air and CO<sub>2</sub> atmosphere. Nevertheless, the slight decrease of apparent density (lower apparent density) and increase of the electrical resistivity could be considered as negative consequence of the removing of the ultrafines. Hulse [48] proposed that the pitch content depends on the fineness of the fine fraction. Indeed, the smaller particles with a high surface area need more pitch to be bound with other particles. This is the reason why, in practice, the pitch demand is determined according to the BN. Thus, with the substitution of the ultrafine particles by larger particles, the anode paste may require less pitch.

In consequence, two different ways to modify the anode recipe are proposed. First, the amount of the truncated fine fraction was increased (+15% relative and +30% relative) while the pitch content was kept constant. Secondly, the pitch content was reduced (-10 % relative and -20% relative), as detailed in Table 9. Table 10 describes the chemical compositions as well as the crystallite size ( $L_C$ ) of the initial anode recipe (4000 BN and 16.2 wt. % of pitch) of the four modified recipes. A second series of the initial recipe was prepared to be in the same conditions than the modified samples. Results show that the augmentation of the fine fraction does not affect significantly the concentration of all chemical elements and the graphitization level of the anodes (the  $L_C$  are quite similar, about 3.0 nm).

**Table 9. Particle size distribution of calcined coke (wt. %) for the four modified anode recipes, made with an amount augmentation of the truncated fine fraction, 53  $\mu\text{m}$  (+ 15% relative and 30% relative of more truncated fine) and a reduction of the pitch content (- 10% relative and 20% relative of less pitch), compared at the initial recipe (4000 BN).**

Type of Fractions		Coarse fraction					
Particle sizes (US Mesh)	Superior Inferior	-4 +8	-8 +14	-14 +28	-28 +50	-50 -100	-100 -200
Particle sizes ( $\mu\text{m}$ )	Superior Inferior	-4760 +2380	-2380 +1410	-1410 +595	-595 +297	-297 +149	-149 +74
Initial particle size distribution		22.0	10.1	11.5	12.7	8.8	10.8
+15% relative fines (+ 53 $\mu\text{m}$ )		21.2	9.6	11.1	12.3	8.5	10.4
+30% relative fines (+ 53 $\mu\text{m}$ )		20.5	9.3	10.7	11.8	8.2	10.1
-10% relative pitch		22.0	10.1	11.5	12.7	8.8	10.8
-20% relative pitch		22.0	10.1	11.5	12.7	8.8	10.8

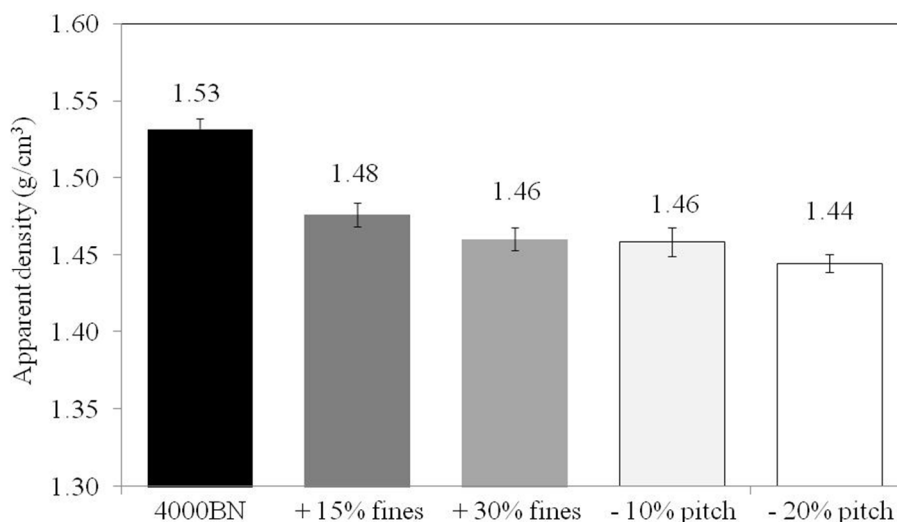
  

Type of Fractions		Fine fraction						Pitch content (wt. %)
Particle sizes (US Mesh)	Superior Inferior	-50 +100	-100 +200	-200 +270	-270 +325	-325 -400	-400	
Particle sizes ( $\mu\text{m}$ )	Superior Inferior	-297 +149	-149 +74	-74 +53	-53 +45	-45 +37	-37	
Initial particle size distribution		1.3	11.8	6.8	0.7	0.4	3.3	16.2
+15% relative fines (+ 53 $\mu\text{m}$ )		1.8	15.9	9.2	0.0	0.0	0.0	16.2
+30% relative fines (+ 53 $\mu\text{m}$ )		1.9	17.4	10.0	0.0	0.0	0.0	16.2
-10% relative pitch		1.3	11.8	6.8	0.7	0.4	3.3	14.6
-20% relative pitch		1.3	11.8	6.8	0.7	0.4	3.3	13.0

**Table 10. Chemical compositions and structural property of the baked anodes made with an amount augmentation of the truncated fine fraction, 53  $\mu\text{m}$  (+ 15% relative and 30% relative of more truncated fine) and a reduction of the pitch content (- 10% relative and 20% relative of less pitch), compared at the initial recipe (4000 BN).**

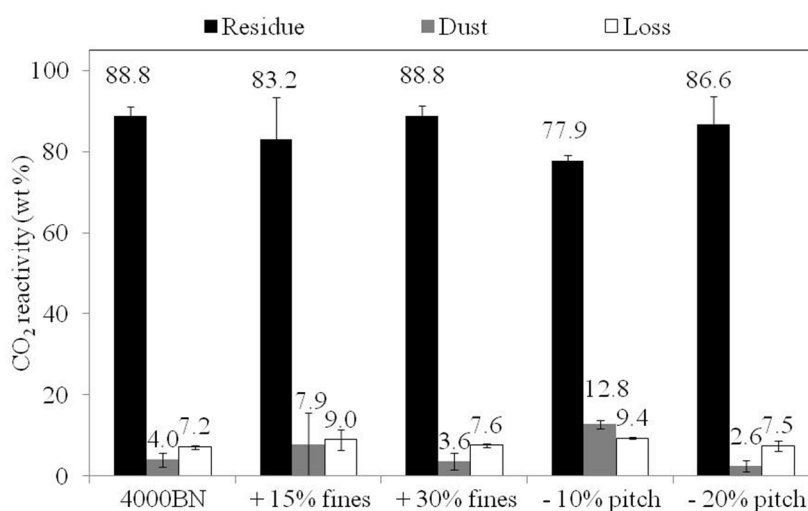
Properties	S (wt %)	Na (ppmw)	Ca (ppmw)	V (ppmw)	Fe (ppmw)	Ni (ppmw)	$L_c$ (nm)
4000BN	1.79 $\pm$ 0.05	104 $\pm$ 7	192 $\pm$ 10	383 $\pm$ 19	635 $\pm$ 32	231 $\pm$ 12	2.9 $\pm$ 0.1
+ 15% relative fines (+ 53 $\mu\text{m}$ )	1.83 $\pm$ 0.05	108 $\pm$ 8	185 $\pm$ 9	392 $\pm$ 20	561 $\pm$ 28	236 $\pm$ 12	3.0 $\pm$ 0.1
+ 30% relative fines (+ 53 $\mu\text{m}$ )	1.86 $\pm$ 0.06	100 $\pm$ 7	183 $\pm$ 9	379 $\pm$ 19	579 $\pm$ 29	229 $\pm$ 11	3.0 $\pm$ 0.1
- 10% relative pitch	1.84 $\pm$ 0.06	117 $\pm$ 8	187 $\pm$ 9	386 $\pm$ 19	686 $\pm$ 34	231 $\pm$ 12	3.0 $\pm$ 0.1
- 20% relative pitch	1.83 $\pm$ 0.05	92 $\pm$ 6	181 $\pm$ 9	388 $\pm$ 19	577 $\pm$ 29	230 $\pm$ 12	3.0 $\pm$ 0.1

As presented previously, the apparent density is a good indicator of the anode quality. Figure 6 presents the variation of the apparent density for five anode recipes; one recipe as a reference with the fine fraction having a BN of 4000; two recipes made with a higher amount of the fine fraction truncated at 53  $\mu\text{m}$  (15 wt. % and 30 wt. % of more truncated fine) and two recipes with a pitch content reduction (10 wt. % and 20 wt. % of less pitch). For both modified recipes of the truncated fine fraction (+15 and +30% of fines), the apparent density was lower than that of the reference anode recipe. The same was observed for the recipes with the decreased pitch content (-10 and -20 wt. %). In consequence, these two modified of recipes are not convenient for the apparent density.



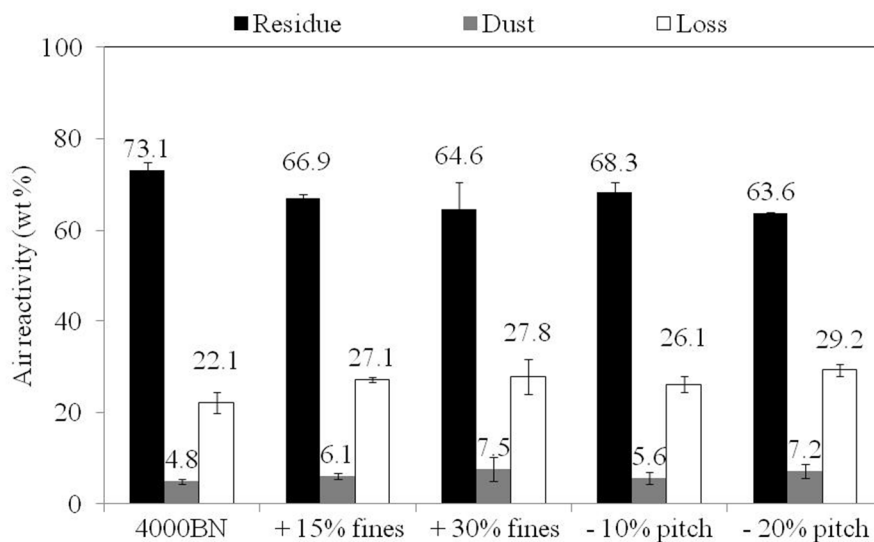
**Figure 6. Apparent density of the baked anodes made with an amount augmentation of the truncated fine fraction, 53  $\mu\text{m}$  (+ 15% relative and 30% relative of more truncated fine) and a reduction of the pitch content (- 10% relative and 20% relative of less pitch), compared at the initial recipe (4000 BN), measured in following the ISO standard 12985-1.**

Air and CO<sub>2</sub> reactivity tests were performed on the modified recipes. Figure 7 presents the CO<sub>2</sub> reactivity of the five types of baked anodes (presented in the table 10). As described in Section 3.1, the CO<sub>2</sub> reactivity is expressed with three parameters; residue, dust and loss. Although, the percentage of residue of the recipe with +30% of fines and -20% of pitch are quite similar compared to the initial recipe, the two other recipes (+15% of fines and -10% of pitch) have a lower residue. The higher CO<sub>2</sub> reactivity of the two recipes (+15% fines and -10% of pitch) is confirmed with higher dust and loss percentages. Conversely, for the two modified recipes (+30% relative of fines and -20% relative of pitch), the dust percentages are lower compared to the initial recipe while the loss percentages are higher. Thus, the two modified recipes did not improve the CO<sub>2</sub> reactivity, however, they slightly decreased the dust emission.



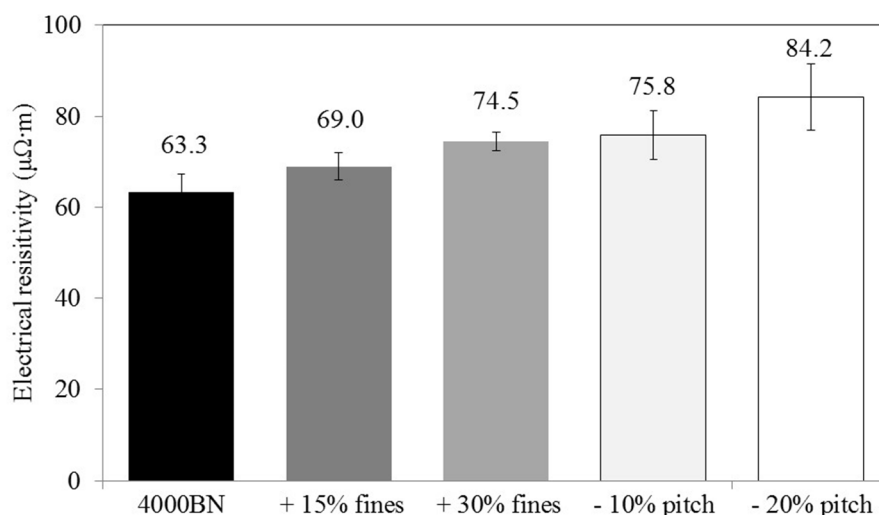
**Figure 7. CO<sub>2</sub> reactivity of the baked anodes made with an amount augmentation of the truncated fine fraction, 53  $\mu\text{m}$  (+ 15% relative and 30% relative of more truncated fine) and a reduction of the pitch content (- 10% relative and 20% relative of less pitch), compared at the initial recipe (4000 BN), measured according to the standard ISO 12988.**

Figure 8 presents the air reactivity of the baked anodes (same composition of anode recipes of the table 10), measured according to the standard ISO 12989-1. Although the recipe adjustments presented some benefic results for CO<sub>2</sub> reactivity, the air reactivity results did not show any improvement for the augmentation of truncated fine fractions and for the pitch reduction. The samples with the modified recipes showed a lower percentage of residues and higher percentages for dust and loss.



**Figure 8. Air reactivity of the baked anodes made with an amount augmentation of the truncated fine fraction, 53  $\mu\text{m}$  (+ 15 wt % and 30 wt % of more truncated fine) and a reduction of the pitch content (- 10 wt % and 20 wt % of less pitch), compared at the initial recipe (4000 BN), measured according to the standard ISO 12989.**

Figure 9 details the electrical resistivity of the modified baked anodes (Table 10) measured according to the Van-der-Pauw method. The two modified recipes show a negative effect on the electrical resistivity of baked anode as for the air reactivity results. This modification on the fines and pitch contents of these samples results on a higher electrical resistivity. Belitskus and Danka [47] and Dreyer et al. [49] reported a similar result for the pitch effect; a diminution of pitch content implies an increasing in the electrical resistivity. Belitskus and Danka [47] proposed also a relationship between the electrical resistivity of anodes and the coke fraction with a particle size comprised between 100 and 200 US Mesh (150 and 75  $\mu\text{m}$ ). The augmentation of the fine content increases the electrical resistivity, most likely due to the decrease in the baked density.



**Figure 9. Electrical resistivity of the baked anodes made with an augmentation of the amount of the truncated fine fraction, 53 μm (+ 15 wt% and 30 wt% of more truncated fine) and a reduction of the pitch content (- 10 wt% and 20 wt% of less pitch), compared at the initial recipe (4000 BN), measured according to the four-probe method.**

#### 4 Conclusion

Ultrafine particles were removed from the fine coke and anode samples were made using the new coke recipe in lab scale. For this purpose, two ways have been proposed: the first one aimed at revealing the effect of removing the finest particles at three levels (particles finer than 37, 45 and 53 μm) on the anode features and the second one aimed at revealing the effect of the quantity of the truncated fine fraction or the reduction of the pitch content.

The substitution of the ultrafine fraction by larger particles has decreased the apparent density and reduced the dust emission during the air reactivity test and resulted in a slight augmentation of the electrical resistivity. The CO<sub>2</sub> reactivity was not affected by the ultrafine substitution. Therefore, considering the important problem of dusting phenomenon in electrolysis pots at an industrial scale, it would be possible to propose a recipe adjustment without modifying all the manufacturing steps.

The augmentation of the truncated fine fraction and the diminution of the pitch content generated several drawbacks; the apparent density and the air reactivity were decreased whereas the electrical resistivity increased. In addition, the CO<sub>2</sub> reactivity has been stabilized for some samples (+30% of fines and - 20% of pitch). Neither the increase in the quantity of the truncated fine coke nor the reduction of pitch content resulted in a better anode quality.

#### Acknowledgments

The authors would like to acknowledge the financial support of Natural Sciences and Engineering Research Council of Canada, Fonds de Recherche du Québec - Nature et Technologies, Alcoa and the Aluminium Research Centre – REGAL. The assistance of Denis Drapeau and his colleagues at Alcoa Deschambault plant (QC, Canada) for conducting the chemical and crystallite size analyses is gratefully acknowledged. The authors would also like to extend their appreciation to Dr. Donald Picard at Laval University for the scientific discussions, as well as Messrs. Jayson Tessier, Guillaume Gauvin and Hugues Ferland for their technical support.

## References

1. Grjotheim, K. and B. Welch, *Aluminium Smelter Technology*, in *Aluminium-Verlag*. 1988: Düsseldorf, Germany.
2. Lustenberger, M., *Heat treatment of anodes for the Aluminium Industry*, in *Institut des matériaux*. 2004, Faculté Sciences et Techniques de l'Ingénieur: Lausanne, Switzerland. p. 143.
3. Tkac, M., *Porosity Development in Composite Carbon Materials during Heat Treatment*, in *Department of Materials Science and Engineering*. 2007, Norwegian University of Science and Technology: Trondheim. p. 189.
4. Tordai, T., *Anode dusting during the electrolytic production of aluminium*. 2007, École Polytechnique Fédérale de Lausanne. p. 351.
5. Fischer, W.K., F. Keller, and R. Perruchoud. *Interdependence between anode net consumption and pot design, pot operating parameters and anode properties*. in *Light Metals 1991*. 1991. New Orleans, United States: TMS.
6. Fischer, F.G., A.R. Feichtinger, and W.K. Fischer, *Carbon reactivity—the combined effect of purity, structure and porous texture on reactivity investigated and generalised by means of the compaction effect*, in *14th Biennial Conference on Carbon*, A.C. Society, Editor. 1979: United States. p. 165.
7. Engvoll, M.A., H.A. Øye, and M. Sørli. *Influence of bath contaminations on anode reactivity*. in *Light Metals 2001*. 2001. New Orleans, USA.
8. Müftüoğlu, T., B. Steine, and R. Fernandez. *Anode Burning Behaviour and Sodium Sensitivity of Coke from Different Feedstocks: A Pilot Scale Study*. in *Light Metals 1993*. 1993. Denver, USA.
9. Müftüoğlu, T. and H. Øye. *Reactivity and electrolytic consumption of anode carbon with various additives*. in *Light Metals 1987*. 1987. Denver, USA.
10. Rolle, J.G. and Y.K. Hoang. *Studies of the impact of vanadium and sodium on the air reactivity of coke and anodes*. in *Light Metals 1995*. 1995. Las Vegas, USA.
11. Buhler, U. and R.C. Perruchoud. *Dynamic process optimization*. in *Light Metals 1995*. 1995. Las Vegas, USA.
12. Coste, B. and J.P. Schneider. *Influence of coke real density on anode reactivity consequence on anode baking*. in *Light Metals 1994*. 1994. San Francisco, USA.
13. Foosnæs, T., et al., *Measurement and control of the calcining level in anode baking furnaces*. Essential Readings in *Light Metals: Electrode Technology for Aluminum Production*, Volume 4, 1995: p. 418-421.
14. Fischer, W.K., et al., *Baking parameters and the resulting anode quality*. Essential Readings in *Light Metals: Electrode Technology for Aluminum Production*, Volume 4, 1993: p. 427-433.
15. Chevarin, F., et al., *Effects of Microstructural Characteristics on Anode Reactivity*, in *COM 2011*. 2011: Montréal, Canada.
16. Chevarin, F., et al., *Active pore sizes during the CO<sub>2</sub> gasification of carbon anode at 960° C*. *Fuel*, 2016. **178**: p. 93-102.
17. Sadler, B.A. and S.H. Algie. *Porosimetric study of sub-surface carboxy oxidation in anodes*. in *Light Metals 1991*. New Orleans, United States.
18. Chevarin, F., et al., *Evolution of Anode Porosity under Air Oxidation: The Unveiling of the Active Pore Size*. *Metals*, 2017. **7**(3): p. 101.
19. Azari, K., et al., *Influence of mixing parameters on the density and compaction behavior of carbon anodes used in aluminum production*, in *Thermec 2012*. 2012, Trans Tech Publ: Quebec city, Canada. p. 17-22.
20. Dreyer, C., B. Samanos, and F. Vogt. *Coke calcination levels and aluminum anode quality*. in *Light Metals 1996*. 1996. Anaheim, United States: TMS.

21. Samanos, B. and C. Dreyer, *Impact of coke calcination level and anode baking temperature on anode properties*. Essential Readings in Light Metals: Electrode Technology for Aluminum Production, Volume 4, 2001: p. 101-108.
22. Belitskus, D., *Effects of mixing variables and mold temperature on prebaked anode quality*. Essential Readings in Light Metals: Electrode Technology for Aluminum Production, Volume 4, 1985: p. 328-332.
23. Azari, K., *Investigation of the materials and paste relationship to improve forming process and anode quality*, in *Mining, Metallurgical and Materials Engineering Department*. 2013, Laval University, Canada. p. 148.
24. Lauzon-Gauthier, J., *Monitoring of a Carbon Anode Paste Manufacturing Process Using Machine Vision and Latent Variable Methods*. 2015, Université Laval.
25. Schmidt-Hatting, W., A. Kooijman, and R. Perruchoud. *Investigation of the quality of recycled anode butts*. in *Light Metals 1991*. 1990. New Orleans, USA.
26. Aga, B.E., et al., *Drilling of stub holes in prebaked anodes*. Essential Readings in Light Metals: Electrode Technology for Aluminum Production, Volume 4, 2003: p. 529-533.
27. Belitskus, D., *Effects of Butts Content, Green Scrap and Used Potlining Additions on Bench-Scale Prebaked Anode Properties*. *Light Metals 1980*, 1980: p. 431-442.
28. Hulse, K.L., et al., *Process adaptations for finer dust formulations: mixing and forming*. Essential Readings in Light Metals, Electrode Technology for Aluminum Production, 2013. **4**: p. 322.
29. Coste, B., *Improving Anode Quality by Separately Optimising Mixing and Compacting Temperature*. Essential Readings in Light Metals: Electrode Technology for Aluminum Production, Volume 4, 1988: p. 333-338.
30. Smith, M.A., *An Evaluation of the Binder Matrix in Prebaked Carbon Anodes Used for Aluminum Production*, in *School of Engineering*. 1991, University of Auckland: Auckland, New Zealand. p. 1986.
31. Vanvoren, C., *Recent improvement in paste plant design industrial application and results*. *Light Metals 1987*, 1987: p. 525-531.
32. Sadler, B.A. and S.H. Algie. *Sub-surface carboxy reactivity testing of anode carbon*. in *Light Metals 1992*. San Diego, United States.
33. Figueiredo, F.E., et al., *Finer fines in anode formulation*. Essential Readings in Light Metals: Electrode Technology for Aluminum Production, Volume 4, 2005: p. 318-321.
34. Jin, X., et al., *Influence of Ultrafine Powder on the Properties of Carbon Anode Used in Aluminum Electrolysis*. *Light Metals 2011*: p. 1141-1147.
35. Stokka, P. and I. Skogland, *Søderberg Paste. Effect of Fine Fraction Variations*. Essential Readings in Light Metals: Electrode Technology for Aluminum Production, Volume 4, 1990: p. 313-317.
36. Majidi, B., et al., *Packing density of irregular shape particles: DEM simulations applied to anode-grade coke aggregates*. *Advanced Powder Technology*, 2015. **26**(4): p. 1256-1262.
37. Majidi, B., et al., *Simulation of vibrated bulk density of anode-grade coke particles using discrete element method*. *Powder Technology*, 2014. **261**: p. 154-160.
38. Azari, K., et al., *Compaction properties of carbon materials used for prebaked anodes in aluminum production plants*. *Powder Technology*, 2013. **246**: p. 650-657.
39. Chevarin, F., et al., *Characterization of carbon anode constituents under CO<sub>2</sub> gasification: A try to understand the dusting phenomenon*. *Fuel*, 2015. **156**(0): p. 198-210.
40. Chevarin, F., et al., *Binder Matrix Reactivity Under CO<sub>2</sub> Gasification: A Possible Explanation Of The Anode Disintegration In The Eletrolysis Bath In Hall-Heroult Process*, in *IMPC 2016, XXVIII International Mineral Processing Congress*, M.a.P.C. Canadian Institute of Mining, Editor. 2016: Quebec City, Canada.
41. Azari, K., et al., *Compaction properties of carbon materials used for prebaked anodes in aluminum production plants*. *Powder Technology*, 2013. **246**(0): p. 650-657.

42. van der Pauw, L., *A method of measuring specific resistivity and Hall effect of discs of arbitrary shape*. Philips Res. Rep, 1958. **13**: p. 1-9.
43. Van der Pauw, L., *A method of measuring the resistivity and Hall coefficient on lamellae of arbitrary shape*. 1958.
44. Rouget, G., et al., *Electrical Resistivity Measurement of Petroleum Coke Powder by Means of Four-Probe Method*. Metallurgical and Materials Transactions B, 2017: p. 1-8.
45. Kasl, C. and M. Hoch, *Effects of sample thickness on the van der Pauw technique for resistivity measurements*. Review of scientific instruments, 2005. **76**(3): p. 033907.
46. Rhedey, P., *A review of Factors Affecting Carbon Anode Consumption in Electrolytic Production of Aluminum*. Journal of Metals 1970, 1970. **22**(12): p. A20.
47. Beltiskus, D. and D. Danka. *A comprehensive determination of effects of calcined petroleum coke properties on aluminium reduction cell anode properties*. in *Light Metals 1988*. 1988. Phoenix, USA.
48. Hulse, K.L., *Anode manufacture: Raw materials formulation and processing parameters*, in *School of Engineering*. 2000, University of Auckland: Auckland, New Zealand. p. 361.
49. Dreyer, C., B. Samanos, and F. Vogt. *Coke calcination levels and aluminum anode quality*. in *Proceedings of the 1996 125th TMS Annual Meeting, February 4, 1996 - February 8, 1996*. 1996. Anaheim, CA, USA: Minerals, Metals & Materials Soc (TMS).

